Pre-operational risk study in deep geothermal modeling:

Insights from a dual medium synthetic model

Morgan Le Lous[12], Alexandre Pryet[1], François Larroque[1], Pierre-Clément Damy[2], Alain Dupuy[1]

[1] Géoressources & Environnement, 1allée F. Daguin, 33607 Pessac Cedex, France

[2] Fonroche Géothermie, ZAC des Champs de Lescaze, 47310 Roquefort, France

morgan.le_lous@ensegid.fr

Keywords: high-enthalpy deep geothermal energy, uncertainty analysis, numerical modeling simulation.

ABSTRACT

Through a multiple realizations approach, two computational methods are retained. By means of Plackett-Burman plans, thorough screening of uncertainties on a given range of input parameters allows the identification of key reservoir simulation outputs due to their respective influence on the functionning of the geothermal system.

This reduced set of parameters will be subsequently used to carry out the uncertainty analysis that enables quantifying parameter impacts on modeled pressures, temperatures and complex output variables, using a Latin Hypercube experimental design.

A meta-model would allow determining the settings for input factors that meet technical feasibility constraints, resulting in the prediction probabilities of success of the overall project.

This integrated work tackles challenges faced in classical stochastic hydrogeological modeling by providing an operational and process-based approach for deep geothermal energy system.

1. INTRODUCTION

A common form of geothermal extraction involves extracting hot water from an aquifer from a production well and re-injecting cooled water in a second injection well within the same aquifer. This system is a typical well-doublet scheme.

Reinjection of cooled water within the reservoir started as a method of wastewater disposal (Sanyal et al. 1995), but has now become one of the key factors in the success or failure of the field. Reinjection provides pressure support, reducing drawdown and the potential for subsidence (Kaya et al. 2011). Also, this process increases the longevity of geothermal resources and the amount of energy that can be recovered (Gringarten and Sauty 1975).

As the operation takes place, a cooled water zone will spread over time from the injection well, eventually reaching the production well. After thermal breakthrough occurs, the outlet temperature is no longer constant, which may have significant consequences for the overall sustainability of the project. Therefore, a careful design of the production–injection system is required for an optimal geothermal development of the field, as well as to prevent an early thermal breakthrough at the production well (Diaz et al. 2016).

The development of geothermal energy generation is closely linked to thermal and hydrogeological knowledge of the subsurface aquifers. Numerical modeling here appears as a tool to delineate development risks induced by limited geological data at great depths.

Computational tools capable of simulating complex geothermal systems coupled to adapted numerical methods of uncertainty design are tailored to evaluate the pre-operational risk associated with the deep geothermal site-specific operation.

2. MODEL DEVELOPMENT

IFPEN in-house reservoir numerical model PumaFlow™ currently commercialized by Beicip Franlab, is used to investigate coupled transient hydraulic and thermal responses of geothermal operation on a deep sloped reservoir.

This reservoir simulator is a three-phase flow model based on mass conservation equations for oil species and water, and Darcy laws for flow modeling coupled with thermodynamic equilibrium equations. A classical fully implicit numerical formulation as well as mixing implicit and explicit time discretisation methods is implemented. These equations are discretised in space with a finite volume scheme and linearized with a Newton-type iterative method (Baroni et al. 2015).

Selected dual medium approach accounts for fractured reservoirs through the modeling of exchange mechanisms between matrix and fractures. We consider here a single phase (water) model.

2.1. Spatial discretization

The geothermal system, consisting of a fully saturated reservoir, overburden and underburden, is assumed to be part of a typical deep sedimentary basin (Fig. 1).

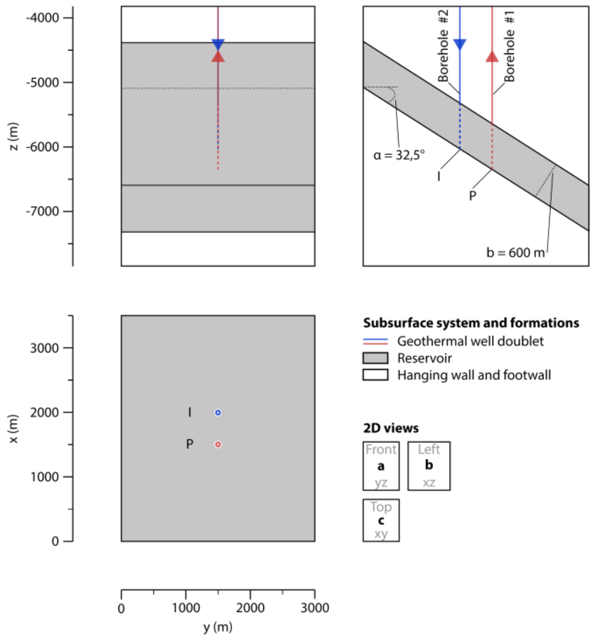

Figure 1: Subsurface formations involved in geothermal well-doublet operation – 2D views of the 3D domain; I: injection well, P: production well, α: reservoir dip, b: reservoir thickness.

The geometrical model consists of a square parallelepiped domain, with dimensions x = 3500 m × y = 3000 m × z = 4030 m. The 3D domain is vertically bounded by two horizontal plans of elevations z = -3821 m and z = -7851, respectively top and bottom surface. The reservoir is 600 m thick. Its top surface (-4366 m ≥ z ≥ -6596 m) has an inclination of 32.5° degrees.

Two vertical wells are located 500 m away at the center of the 3D domain: one water injector (borehole #1) at point I (x = 2000 m; y = 1500 m) and one producer (borehole #2) at point P (x = 1500 m; y = 1500 m). Their openhole sections are 712 m long, located from z = -5321 m to z = - 6033 m for the injection well and from -5640 m and z = -6351 m for the production well.

The 3D spatial discretization is achieved by means of a local grid refinement (Fig.2, Table 1). Three embedded local models (coloured meshes), referred to as children models, are coupled to a larger regional model, called parent model (black mesh, Fig. 2).

The purpose of the parent model is to provide the boundary conditions from the parent model to the children models that are consistent with the regional flow system. The function of the children models is to simulate phenomena that require a finer mesh than the parent contains, as we expect sharp changes in pressure and temperature gradients at the vicinity of both wells (Mehl and Hill 2002).

Parent mesh is made of parallelepipeds with dimensions 100 m. Children meshes are obtained by splitting the parent mesh by 2, 4 and 8 leading to respectively 50 m, 25 m and 12.5 m parallelepipedic meshes, with finer discretization at the center of the geometrical domain.

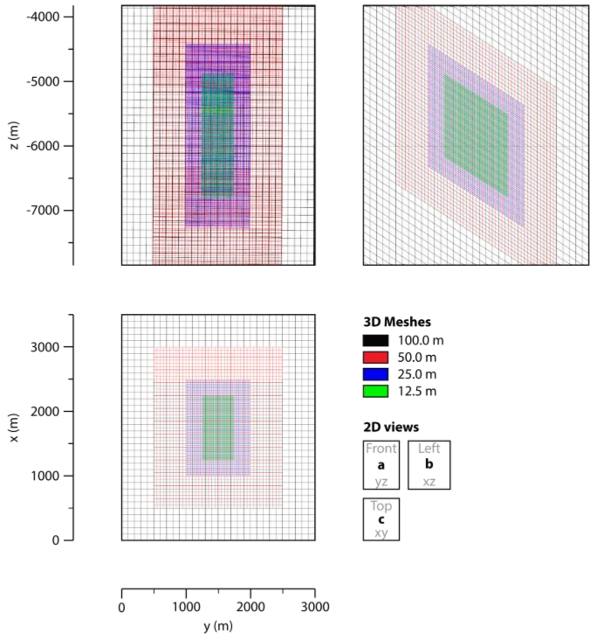

Figure 2: Parent (100 m) and children meshes (50 m, 25 m and 12.5 m) involved in numerical simulation – 2D views of the 3D domain.

2.2. Boundary and initial conditions

The hypothetic flow and heat conditions emerge from the steady-state boundary conditions. The reservoir and confining beds terminate horizontally in hydraulic and thermal no-flow boundaries.

Fixed pressure boundary conditions (Dirichlet type) of 382.1 bars, set at the elevation of -3821 m, yield as hydrostatic initial pressure in the 3D domain in absence of regional groundwater flow for the reference case.

The heat boundary conditions provide an average geothermal gradient of 0.03 $K.m^{-1}$, within the range of typical values (0.03–0.06 Km^{-1}) observed in Europe (Stober and Bucher 2014). Constant temperature boundary conditions (Dirichlet type) of 124.6 °C and 245.5°C apply respectively to the top and bottom of the 3D domain for the reference case.

The production schedule is defined over 30 years. Injecter and producer are imposed a 0.125 m^3/second rate (450 m^3/h) for the reference case. The flowrate constraint is changed to a bottomhole pressure (BHP) control when BHP rises above 1000 bars for injecter and drops below 1 bar for producer. A radius of 0.15 m is used for both injection and production wells within the openhole sections. For the reference case, the injection of cooled geothermal fluids occurs at a fixed temperature of 65 °C. At 1 day of simulation time, 200 kg of fluorescein disodium salt is performed within 3 hours at the injecter to illustrate hydraulic and chemical communications between the injection and production wells.

Brine concentration in total dissolved solids (TDS) is assumed to be 100 $kg.m^{-3}$ in the entire domain, within the range of typical values encountered in the Upper Rhine Graben (San Juan, 2010). Viscosity and density dependencies to salt concentration, not treated explicitly in the numerical modeling, are directly implemented in the corresponding equations of state.

Table 1: Properties related to the local grid refinement process for parent model (100 m) and children meshes (50 m, 25 m and 12.5 m); N_i: Cell number and L_i: total length of the mesh along the i-axis; I_{min} and I_{max}: minimum and maximum cartesian coordinates of the mesh along the i-axis, respectively.

Mesh	100 m	50 m	25 m	12.5 m
Cell number	63000	104000	153600	281600
N_x	35	50	60	80
N_y	30	40	40	40
N_z	60	52	64	88
L_x (m)	3500	2500	1500	1000
X_{min} (m)	0	500	1000	1250
X_{max} (m)	3500	3000	2500	2250
L_y (m)	3000	2000	1000	500
Y_{min} (m)	0	500	1000	1250
Y_{max} (m)	3000	2500	2000	1750
L_z (m)	4030	4030	2853	1942
Z_{min} (m)	-7851	-7851	-7263	-6807
Z_{max} (m)	-3821	-3821	-4410	-4866

3. MODEL ANALYSIS

3.1 Motivations

Deep geothermal targets are generally located within complex geological systems, such as multi-scale fault zones, generally characterized by a strong spatial variability of many of its spatially distributed properties among which permeability, porosity, compressibility, thermal conductivity, volumetric heat capacity.

The development of geothermal energy generation is closely linked to thermal and hydrogeological knowledge of the subsurface aquifers. Numerical modeling here appears as a tool to delineate development risks induced by limited geological data at great depths.

CougarFlow™ is an extensive uncertainty and optimization analysis software. With third-party simulator PumaFlow™, it constitutes a reservoir modeling chain capable of investigating effects of input parameters on simulation results.

3.2 Principle

The analysis of numerical studies related to geothermal operation is often limited by the computational cost associated with the complexity, the size and the spatial discretization of the geometrical models as well as the large number of factors or variables to be studied (Tinsson 2010). The approximation of a numerical model by a statistical model (surrogate model) is an effective way to improve the management of uncertainties as well as the optimization of the probabilities of success associated with deep geothermal projects.

A generic method for modeling the behavior of an unknown function $y = f(\boldsymbol{x})$, represented by a black box, consists in collecting the scalar outputs (or responses) $y^{(1)}, y^{(2)},..., y^{(n)}$ resulting from an input vector $\boldsymbol{x}^{(1)}, \boldsymbol{x}^{(2)},..., \boldsymbol{x}^{(n)}$ then find the best estimate $\hat{f}(\boldsymbol{x})$ of the response function of the black box f, based on these known observations (Forrester et al. 2008). This black box can take the form of a physical or computer experience, for example a finite element code, which allows the computation of the maximum stress *(f)* for given product dimensions *(**x**)*. The approximation of a function is usually done in three steps:

- sample an N number of samples within the definition domain $\mathbb{D}$ of the function $y = f(\boldsymbol{x})$,
- evaluate the function at these points,
- use an approximation method to approach the function over the entire experimental domain.

The objective of experimental designs is to choose the best possible experiments to discover the rules of evolution of a quantity of interest according to random factors. Classical designs are full (Fisher 1937, Fisher 2006) or fractional factorial (Goupy 1990), Plackett-Burman (Plackett and Burman 1946), central composite (Cuthbert and Wood 1980), Box–Behnken (Box and Draper 1987) and Doehlert (Doehlert 1970). The designs differ in how the factors are varied and the number of experimental runs that have to be completed (Nicholls et al. 2016). The experiment is then represented by a point in a limited region of the experimental space (Fig. 3).

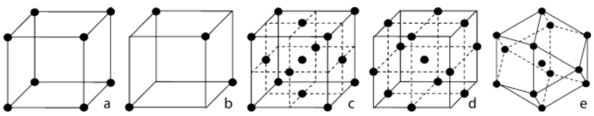

Figure 3: Schematic illustration of the experimental designs commonly used. Points represent experimental runs of a three factor (a) full factorial, (b) fractional factorial, (c) central composite, (d) Box–Behnken, and (e) Doehlert design (Nicholls et al. 2016).

To understand the effect of interactions between various independent parameters, a complete factorial design could be used. A two-level full factorial design, comprising all possible combinations of selected high and low values for the parameters, would require $N = 2^{10} = 1024$ simulations for as few as $k = 10$

parameters. The use of a 1/4 fractional factorial experimentation could reduce the number down to N = 2^8 = 256 experiments.

3.3 Method

In this work, k = 37 parameters are considered of potential interest on geothermal operation (Table 2). Due to the large number of factors studied (and induced simulations), it is often inconvenient in practice to study all combinations of parameters. Under these conditions, other methods can correctly quantify the main effects and/or the estimation of interaction effects between parameters at lower computational cost.

Through a multiple realizations approach based on experimental design and state of the art optimization algorithms, two computational methods are retained. Plackett-Burman plan allows the identification of key reservoir simulation inputs from most of factors involved in the numerical modeling of deep geothermal operation. Stratified design, applied on a reduced set of parameters, then enables to quantify parameter impacts on modelled pressures, temperatures as well as complex output variables.

Based on the results of the steady-state study, the hydraulic, chemical and thermal comportments of the geothermal doublet operation were investigated in terms of transient bottom hole pressure (BHP), tracer component mass rate (TCMR) and bottomhole temperature (BHT) over 30 years of operation.

To compare the effect of a parameter change on the hydraulic and thermal functioning of the well doublet, the BHT series at points P as well as BHP series at points P and I were computed for each simulation after 30 years of operation.

To delineate the hydraulic and chemical relation existing between the injection and production wells, the breakthrough time (TBT, time for 5% the tracer maxima to pass the sampling point P) as well as the ratio of the mean time (time for half the tracer to pass the sampling point P) and the modal time (time to reach peak tracer concentration) are calculated from the TCMR series at production well. This ratio is hereafter called index of tracer asymmetry (TAI).

3.4 Plackett-Burman design

We realized a thorough screening of uncertainties on a given range of input parameters, using a very economical, two-level design called Plackett-Burman. Sample size being a multiple of four, a design with N samples can be used to study up to $k = N - 1$ parameters. This qualitative step is used to organize the main characteristics of the mining reservoir and the associated geothermal operation into a hierarchy in order to discard minor parameters from further (and time-consuming) analysis.

In this work, 37 parameters lead to 40 experimental sample points. Input parameters are related to (Table 3):

- rock properties: compressibility, permeability with respect to the i-axis, porosity, matrix block size with respect to the i-axis, thermal conductivity, specific heat capacity,
- subsurface initial conditions: initial top pressure of the trap and temperature gradient coming from top and bottom thermal boundary conditions,
- operational design: productivity or injectivity indexes, discharge rate, injection temperature.

Table 2: Naming convention used for the identification of parameters.

Latin and greek		Sub/superscripts	
c	compressibility	bot	bottom of domain
k	permeability	f	fracture
M	multiplying factor	II	injectivity index
P	pressure	m	matrix
Q	flowrate	PI	productivity index
s	block size	r	reservoir
T	temperature	top	top of domain
λ	thermal conductivity	w	wall
ρc	vol. heat capacity	x, y, z	coordinate
ω	porosity		

To fully capture the role of the subsurface factors on specific outputs, some parameters are anisotropic (permeability, block size), spatially distributed to reservoir hanging/footwalls (e.g. thermal conductivity, volumetric heat capacity…) and selectively applied to fracture or matrix (e.g. porosity, compressibility…). Pressure and temperature gradients, initial subsurface conditions, are also part of this study (top/bottom thermal and top hydraulic boundary conditions).

To compare uncertainties associated to natural properties versus anthropic design, some parameters are related to the geothermal operation (injection temperature, flowrate) and well hydraulic connection to the reservoir (productivity/injectivity indexes) that can be, for example, increased by specific stimulations *(M > 1)* or altered by the precipitation of dissolved component in brines over circulation time *(M < 1)*.

Table 3: Parameters examined in the sensitivity analysis and their upper/lower bounds. A black dot indicates key parameters selected for the quantitative step realized by latin hypercube sampling.

Parameter		Unit	Lower bound	Upper bound
c_f^r		bar^{-1}	1.00×10^{-5}	1.00×10^{-3}
c_f^w		bar^{-1}	1.00×10^{-4}	1.00×10^{-2}
c_m^r		bar^{-1}	1.00×10^{-6}	1.00×10^{-4}
c_m^w		bar^{-1}	1.00×10^{-5}	1.00×10^{-3}
$k_{x,f}^r$	•	mDa	$1.00\times10^{+0}$	$1.00\times10^{+2}$
$k_{x,f}^w$	•	mDa	1.00×10^{-1}	$1.00\times10^{+1}$
$k_{x,m}^r$	•	mDa	1.00×10^{-1}	$1.00\times10^{+1}$
$k_{x;m}^w$	•	mDa	1.00×10^{-1}	$1.00\times10^{+1}$
$k_{y,f}^r$	•	mDa	$1.00\times10^{+0}$	$1.00\times10^{+2}$
$k_{y,f}^w$	•	mDa	1.00×10^{-1}	$1.00\times10^{+1}$
$k_{y,m}^r$	•	mDa	1.00×10^{-1}	$1.00\times10^{+1}$
$k_{y,m}^w$	•	mDa	1.00×10^{-1}	$1.00\times10^{+1}$
$k_{z,f}^r$	•	mDa	$1.00\times10^{+0}$	$1.00\times10^{+2}$
$k_{z,f}^w$	•	mDa	1.00×10^{-1}	$1.00\times10^{+1}$
$k_{z,m}^r$	•	mDa	1.00×10^{-1}	$1.00\times10^{+1}$
$k_{z,m}^w$	•	mDa	1.00×10^{-1}	$1.00\times10^{+1}$
M_{II}	•	1	5.00×10^{-1}	$1.00\times10^{+1}$
M_{PI}	•	1	5.00×10^{-1}	$1.00\times10^{+1}$
P_{top}	•	bar	$4.11\times10^{+2}$	$4.54\times10^{+2}$
Q	•	$m^3\,d^{-1}$	$9.72\times10^{+3}$	$1.19\times10^{+4}$
s_x^r		m	1.00×10^{-2}	$1.00\times10^{+0}$
s_x^w		m	1.00×10^{-1}	$1.00\times10^{+1}$
s_y^r		m	1.00×10^{-2}	$1.00\times10^{+0}$
s_y^w		m	1.00×10^{-1}	$1.00\times10^{+1}$
s_z^r		m	1.00×10^{-2}	$1.00\times10^{+0}$
s_z^w		m	1.00×10^{-1}	$1.00\times10^{+1}$
T_{bot}	•	°C	$2.25\times10^{+2}$	$2.36\times10^{+2}$
T_{inj}		°C	$5.85\times10^{+1}$	$7.15\times10^{+1}$
T_{top}		°C	$1.36\times10^{+2}$	$1.43\times10^{+2}$
λ^r		$J\,m^{-1}\,s^{-1}\,K^{-1}$	$3.00\times10^{+0}$	$3.50\times10^{+0}$
λ^w		$J\,m^{-1}\,s^{-1}\,K^{-1}$	$2.20\times10^{+0}$	$3.10\times10^{+0}$
$\rho^r c^r$		$MJ\,m^{-3}\,K^{-1}$	$1.80\times10^{+0}$	$2.20\times10^{+0}$
$\rho^w c^w$		$MJ\,m^{-3}\,K^{-1}$	$1.30\times10^{+0}$	$2.00\times10^{+0}$
ω_f^r	•	1	1.00×10^{-4}	1.00×10^{-2}
ω_f^w	•	1	1.00×10^{-4}	1.00×10^{-2}
ω_m^r	•	1	1.00×10^{-3}	1.00×10^{-1}
ω_m^w	•	1	1.00×10^{-3}	1.00×10^{-1}

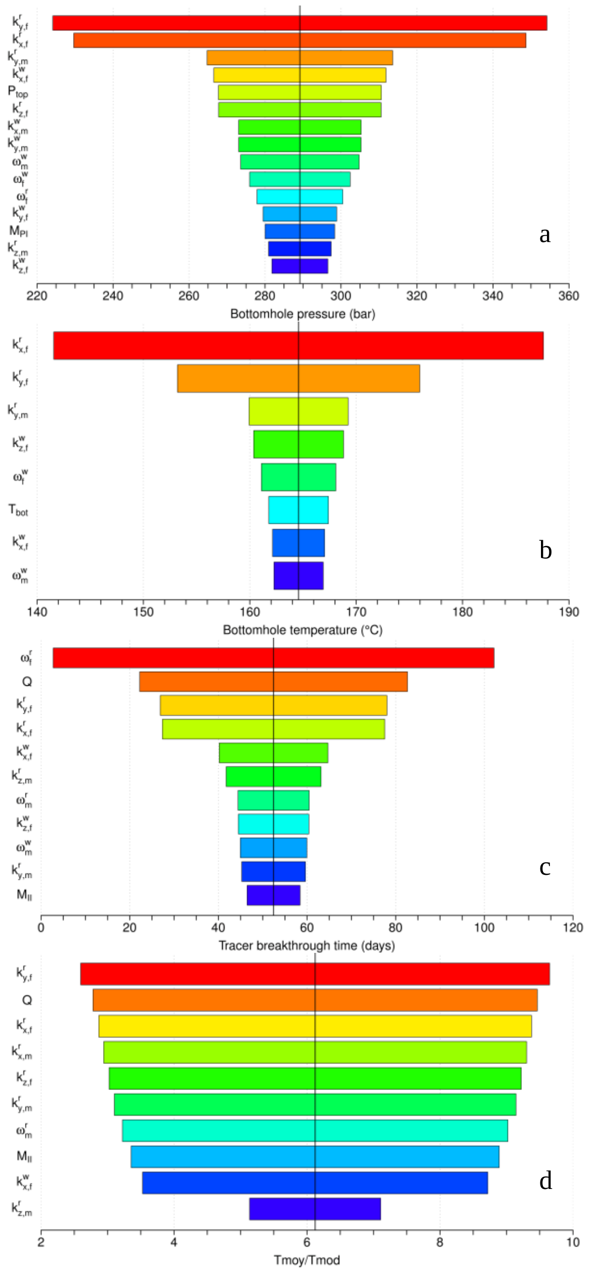

Figure 4: Tornado plots related to (a) BHP, (b) BHT, (c) TBT and (d) TAI at production well. Selected input factors lead to contribution higher than 10 %.

Initial BHP at wells ranges from 366 to 410 bars, depending on the P_{top} value. The median values of the final BHP are 330 bars and 454 bars, respectively at points P and I. Final BHP ranges are 34-401 bars at the producer and 331-1000 bars at the injecter. Input factors controlling BHP response at wells are very similar as injecter and producer share 14 out of 15 of the most important ones (Fig. 4, Table 4). Among these, permeabilities of the reservoir ($k_{x,f}^r$, $k_{y,f}^r$, $k_{y,m}^r$, $k_{z,f}^r$) are the key parameters, affecting the pressure at wells the most. To a lesser extent, fracture and matrix horizontal permeabilities of the walls ($k_{x,f}^w$, $k_{x,m}^w$, $k_{y,m}^w$, $k_{y,f}^w$) are of secondary importance. Hydraulic initial regime (P_{top}) is also involved in the alteration of the hydraulic response of the reservoir. At the exception of M_{PI}, no operational parameters appear of major influence.

Initial production temperature ranges from 195 to 205°C, depending on the T_{top} and T_{bot} values. Minimal and maximal final BHT values are respectively 112 and 195°C, according to the recycle water volume from the injection well. The key parameters are the horizontal permeabilities of the reservoir ($k_{x,f}^r$, $k_{y,f}^r$, $k_{y,m}^r$). Permeabilities of the walls are of secondary interest in terms of thermal breakthrough time ($k_{z,f}^w$, $k_{x,f}^w$). To a lesser extent, the porosity of the aquitard affects thermal transport between wells (ω_f^w, ω_m^w). Finally, initial thermal conditions may alter final BHT at the production well (T_{bot}).

Table 4: Ranking order (from 1 to 15) of input parameters selected in regards of a contribution in BHP, BHT, TBT or TAI higher than 10 %.

	P				I
Parameters	BHP	BHT	TBT	TAI	BHP
$k_{x,f}^r$	2	1	4	3	1
$k_{x,f}^w$	4	7	5	9	4
$k_{x,m}^r$				4	
$k_{x,m}^w$	7				8
$k_{y,f}^r$	1	2	3	1	2
$k_{y,f}^w$	12				11
$k_{y,m}^r$	3	3	10	6	3
$k_{y,m}^w$	8				7
$k_{z,f}^r$	6			5	5
$k_{z,f}^w$	15	4	8		13
$k_{z,m}^r$	14		6	10	12
$k_{z,m}^w$					
M_{II}			11	8	
M_{PI}	13				
P_{top}	5				10
Q			2	2	
T_{bot}		6			
ω_f^r	11		1		14
ω_f^w	10	5			6
ω_m^r			7	7	
ω_m^w	9	8	9		9

Tracer breakthrough time (TBT) occurs from 0.1 day to 405 days, according to hydraulic communication between wells. Through this multiple realization process, the value of the index of the tracer asymmetry (TAI) increases from 1 to 52, as the mean time being delayed from the modal time (asymmetric peak on the tracer concentration curves). A value of TAI much higher than 1 emphases the important role of the secondary porosity through the mass exchange between the matrix and fractures cells. Key parameters are related to the hydraulic comportment between wells mainly dictated by the flowrate (Q) and the horizontal fracture permeabilities of the reservoir ($k_{x,f}^r$, $k_{y,f}^r$). Reservoir porosities play also an important role as it conditioned water displacement within porous media (ω_f^r, ω_m^r).

This qualitative step allows the identification of key reservoir simulation outputs due to their respective influence on hydraulic and thermal performances of the geothermal system. According to their respective contribution to multiple output variables, 21 inputs factors (out of 37 from the complete Plackett-Burman plans) are selected to be further studied as they may control the overall success of the geothermal project.

With Plackett-Burman design, main effects of individual factors are separate from each another, but may be impossible to distinguish from some 2-way interaction effects (aliasing). Therefore, this method is generally restricted to the assessment of large main effects that will be further described with a quantitative method base on stratified design.

3.5 Latin Hypercube design

The sensitivity study is conducted by stratified sampling on a reduced sample dimension of 21 parameters, which consists in dividing the population into disjoint subspaces or strata, and then sampling randomly within each of these subspaces. Latin Hypercube Sampling (LHS) is a special case of stratified sampling for which the division is carried out according to equiprobable subspaces, sampled uniformly. In LHS designs, there is only one sample in each row and each column (Fig. 5). This technique has been described in (McKay et al. 1979) and analyzed in (Iman and Conover 1980, Stein 1987, Owen 1997).

This reduced set of parameters is subsequently used to carry out the uncertainty analysis that enables quantifying parameter impacts on modeled pressures, temperatures and complex output variables. Model execution being time-consuming, the use of response surface method allows simulating thousands of automated scenarios using a latin hypercube experimental design and a response surface approach.

The analysis of this new design, made of 150 experiments, is still under development and will be part of the oral presentation that will be held in The Hague.

Results should allow distinguishing parameter interactions from main effects that are aliased for the

Plackett-Burman method. Results are expected, not only to confirm the important role of the parameters highlighted in the first instance, but also to significantly delineate the shapes of the validated surface responses of BHP, BHP, TBT and TAI. Based on the stochastic method, this meta-model would allow determining the settings for input factors that meet technical feasibility constraints, resulting in the prediction probabilities of success of the overall project (Mottaghy et al. 2011).

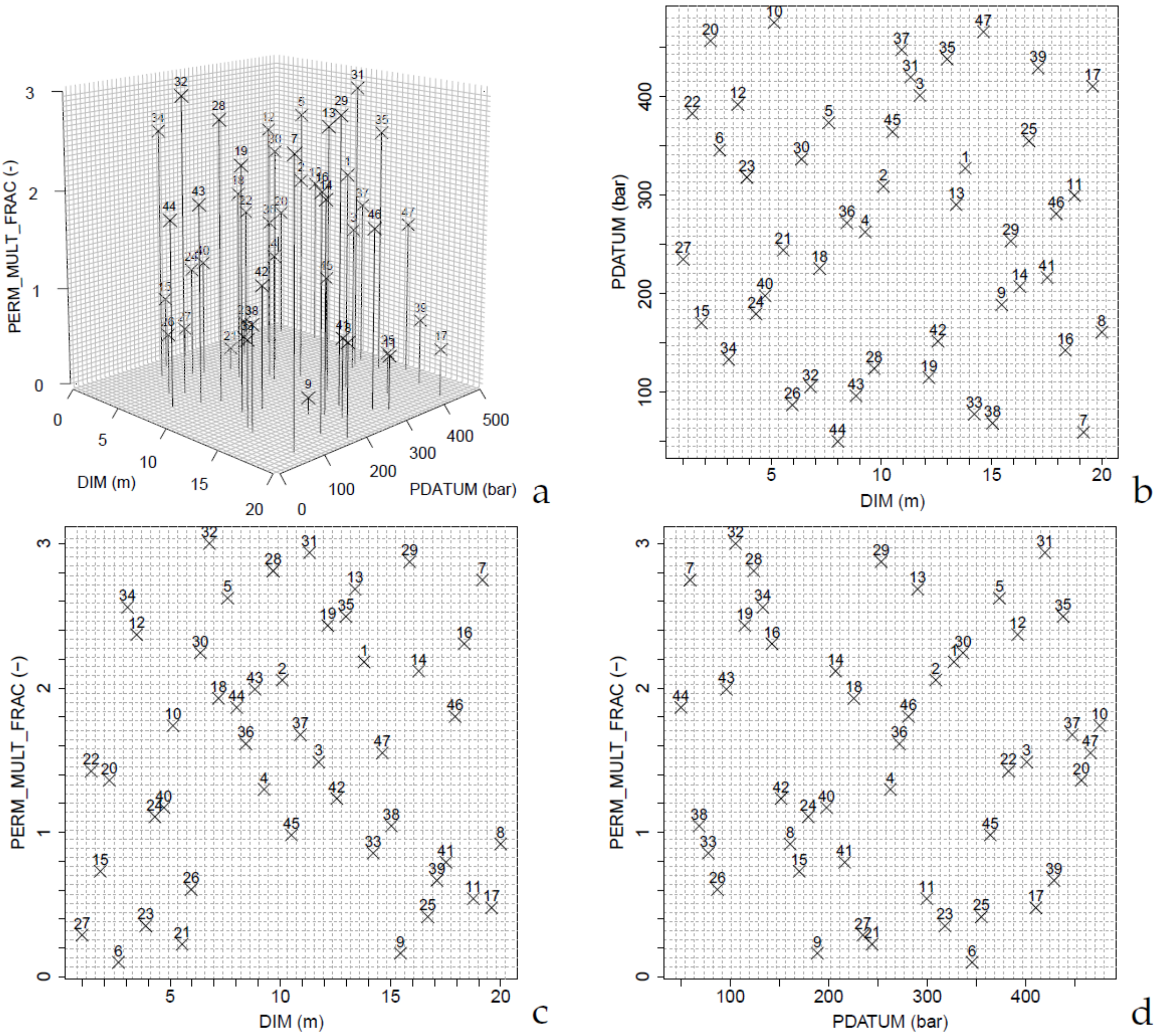

Figure 5: (a) Example of a three-dimensional Latin hypercube design with 47 points and (b, c, d) related two-dimensional projections.

4. CONCLUSIONS

This paper presents the study, through a numerical approach, of a liquid-dominated high-enthalpy geothermal well doublet located in a deep fractured reservoir, overburden and underburden by confining beds.

Through a Plackett-Burman experimental design, a fully coupled thermo-hydro numerical modelling has been used to organize the main characteristics of the double porosity reservoir and the associated geothermal operation into a hierarchy. The hydraulic, chemical and thermal influence of the reservoir, hanging and footwalls are determined through the calculating of BHP, BHT, TBT and TAI at both production and injection wells.

Subsurface key parameters are fracture and matrix permeabilities and porosities. Initial conditions (pressure and thermal vertical distributions) cannot be neglected. Main operational parameters are the flowrate as well as the productivity and injectivity indexes.

Using these results, investors may further calculate the financial risk, and operators may adjust their exploitation strategy for the entire life-cycle of the reservoir based on a quantitative approach, using state-of-the-art Latin Square designs (Hamon et al. 1991).

This integrated work tackles challenges faced in classical stochastic hydrogeological modeling by providing an operational and process-based approach for deep geothermal energy system.

REFERENCES

Baroni, A., Estublier, A., Vincké, O., Delprat-Jannaud, F. and Nauroy, J.-F.: Dynamic fluid flow and geomechanical coupling to assess the CO2 storage integrity in faulted structures; *Oil & Gas Science and Technology-Revue d'IFP Energie nouvelles*, **70(4)**, (2015), 729-751.

Box, G.E.P. and Draper, N.R.: Empirical model-building and response surfaces, *John Wiley & Sons* (1987).

Cuthbert, D. and Wood, F.S.: Fitting Equations to Data: Computer Analysis of Multifactor Data, John Wiley & Sons, Inc., New York, (1980).

Diaz, A.R., Kaya, E. and Zarrouk, S.J. Reinjection in geothermal fields – a worldwide review update, *Renewable and Sustainable Energy Reviews*, **53**, (2016), 105-162.

Doehlert, D.H.: Uniform shell designs, *Applied statistics*, (1970), 231-239.

Fisher, R.A.: The design of experiments, *Oliver And Boyd*; Edinburgh, (1937).

Fisher, R.A.: Statistical methods for research workers. *Genesis Publishing Pvt Ltd*, (2006).

Forrester, A., Sobester, A. and Keane, A.: Engineering design via surrogate modelling: a practical guide, *John Wiley & Sons*, (2008).

Goupy, J. : Étude comparative de divers plans d'expériences, *Revue de statistique appliquée*, **38.4**, (1990), 5-44.

Gringarten, A. and Sauty, J.-P.: A theoretical study of heat extraction from aquifers with uniform regional flow, *Journal of Geophysical Research*, **80(35),** (1975), 4956-4962.

Hamon, G., Mauduit, D., Bandiziol, D. and Massonnat, G.: Recovery optimization in a naturally fractured water-drive gas reservoir: meillon field. *SPE Annual Technical Conference and Exhibition*, (1991), Society of Petroleum Engineers.

Iman, R.L. and Conover, W.J.: Small sample sensitivity analysis techniques for computer models with an application to risk assessment, *Communications in statistics-theory and methods*, **9(17)**, (1980), 1749-1842.

Kaya, E., Zarrouk, S.J. and O'Sullivan, M.J.: Reinjection in geothermal fields: a review of worldwide experience, *Renewable and Sustainable Energy Reviews*, **15(1)**, (2011),47-68.

McKay, M.D., Beckman, R.J. and Conover, W.J.: Comparison of three methods for selecting values of input variables in the analysis of output from a computer code, *Technometrics*, **21(2)**, (1979), 239-245.

Mehl, S. and Hill, M. C.: Development and evaluation of a local grid refinement method for block-centered finite-difference groundwater models using shared nodes, *Advances in Water Resources*, ***25*(5)**, (2002), 497-511.

Mottaghy, D., Pechnig, R. and Vogt, C.:. The geothermal project Den Haag: 3D numerical models for temperature prediction and reservoir simulation, *Geothermics*, **40(3)**, (2011), 199-210.

Nicholls, I.A., Andersson, H.S., Golker, K., Henschel, H., Karlsson, B.C., Olsson, G.D., Rosengren, A.M, Shoravi, S., Suriyanarayanan, S., Wiklander, J.G and Wikman, S.: Rational design of biomimetic molecularly imprinted materials: theoretical and computational strategies for guiding nanoscale structured polymer development, *Analytical and bioanalytical chemistry*, **400(6)**, (2011), 1771.

Owen, A. B. (1997). Monte Carlo variance of scrambled net quadrature. SIAM Journal on Numerical Analysis, 34(5), 1884-1910.

Plackett, R.L. and Burman, J.P.: The Design of Optimum Multifactorial Experiments, *Biometrika*, **33.4**, (1946), 305-325.

Sanjuan, B., Millot, R., Dezayes, C. and Brach, M.: Main characteristics of the deep geothermal brine (5 km) at Soultz-sous-Forêts (France) determined using geochemical and tracer test data, *Comptes Rendus Geoscience*, **342**, (2010), 546-559.

Sanyal, S.K., Granados, E.E. and Menzies, A.J.: Injection-related problems encountered in geothermal projects and their mitigation: the United States experience. *World Geothermal Congress 1995*, Florence, Italy, (1995), 2019-2022.

Stein, M.: Large sample properties of simulations using Latin hypercube sampling, *Technometrics*, **29(2)**, (1987), 143-151.

Stober, I. and Bucher, K.: Hydraulic and hydrochemical properties of deep sedimentary reservoirs of the Upper Rhine Graben, Europe, *Geofluids*, **15**, (2014), 464-482

Tinsson, W.: Plans d'expérience : constructions et analyses statistiques, *Springer Science & Business Media*, (2010).

Acknowledgements

This research is carried out in the REFLET – GEODENERGIES project handled by Fonroche Géothermie.